# Investigation of silicon strip sensors and alternative powering concepts for the ATLAS upgrade

Marçà Josep Boronat Arévalo
Facultat de Física, Universitat de València

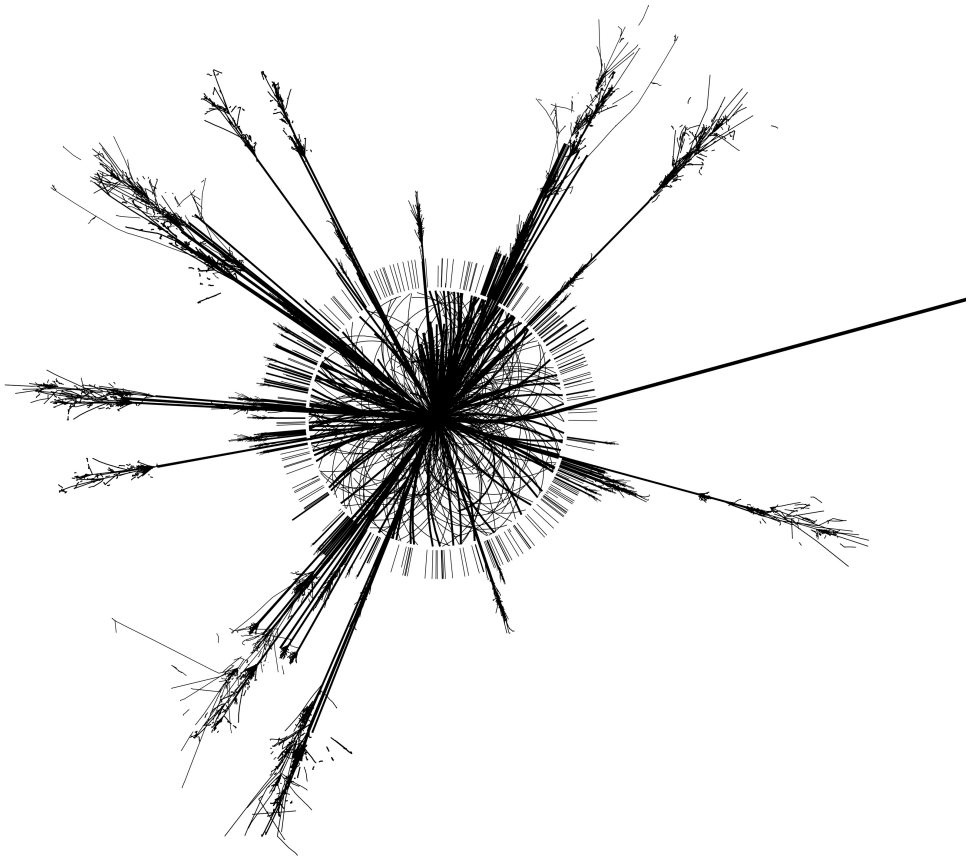

**-DESY, Zeuthen Site-**
**Summer Student Programme**

Supervised by Conrad Friedrich, Hongbo Zhu and Ulrich Husemann

# Contents

# 1 Introduction

In this report I will summerize my work in the ATLAS group during my stay at DESY, where the topics I have worked on consisted of **characterization of silicon sensors for the ATLAS SCT upgrade**, **noise susceptibility tests of the ATLAS pixel front-end electronics** and **investigation of piezoelectric transformers**. In the following sections I will briefly introduce the Large Hadron Collider (LHC) and the ATLAS experiment, followed by a motivation and presentation of results obtained from the measurements done within the mentioned projects.

# 2 LHC and ATLAS experiment

## 2.1 LHC

The LHC is the largest particle collider ever built. It is situated at the European Organization for Nuclear Research (CERN) near Genève, at the Franco-Swiss border. It consists of a 27 km long accelerator ring and four different detectors (ALICE, LHCb, CMS and ATLAS) placed in 4 caverns aproximately 100 m under ground. Inside the LHC, bunches of protons at discrete intervals of 25 ns will be accelerated to 7 TeV, and collided head-on at the center-of-mass energy of $\sqrt{s} = 14$ TeV. The design luminosity is $10^{34}$ cm$^{-2}$s$^{-1}$.

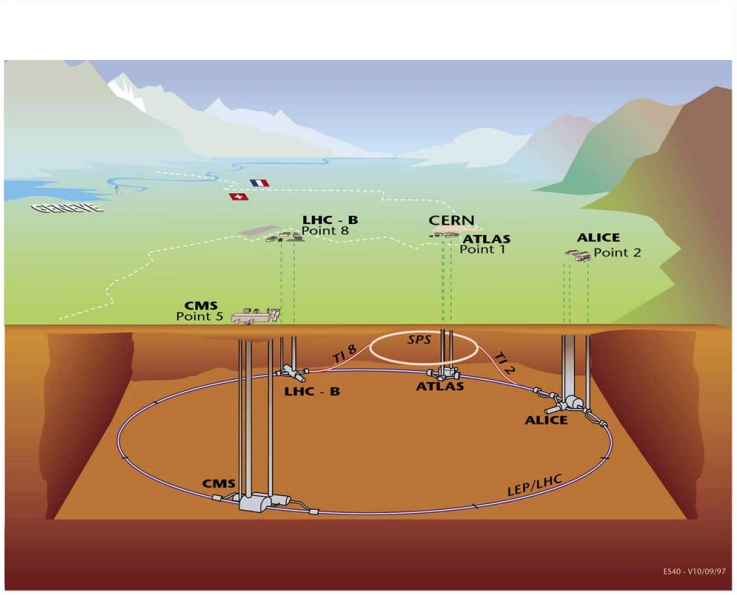


Figure 1: Overall view of the LHC experiment [1]

Currently the machine is running at an energy of $\sqrt{s} = 7$ TeV with an instantaneous luminosity of $10^{31}$ cm$^{-2}$s$^{-1}$.
Among the four mentioned detectors CMS and ATLAS are large multi-purpose detectors, optimized for the search for the Higgs boson and the study of physics beyond the Standard Model. ALICE is built to study the physics of heavy ion collisons and LHCb optimized for $b$-physics studies.

## 2.2 ATLAS experiment

The ATLAS detector is the largest paticle physics detector ever built. It is a huge cilindrical detector of 22 meters in diameter, 45 meters in length and 7000 tons in weight. Around 3000 scientists and engineers from over 30 countries work on this project.
The ATLAS detector consists of many components, built to measure different types of particles produced in the collisions.

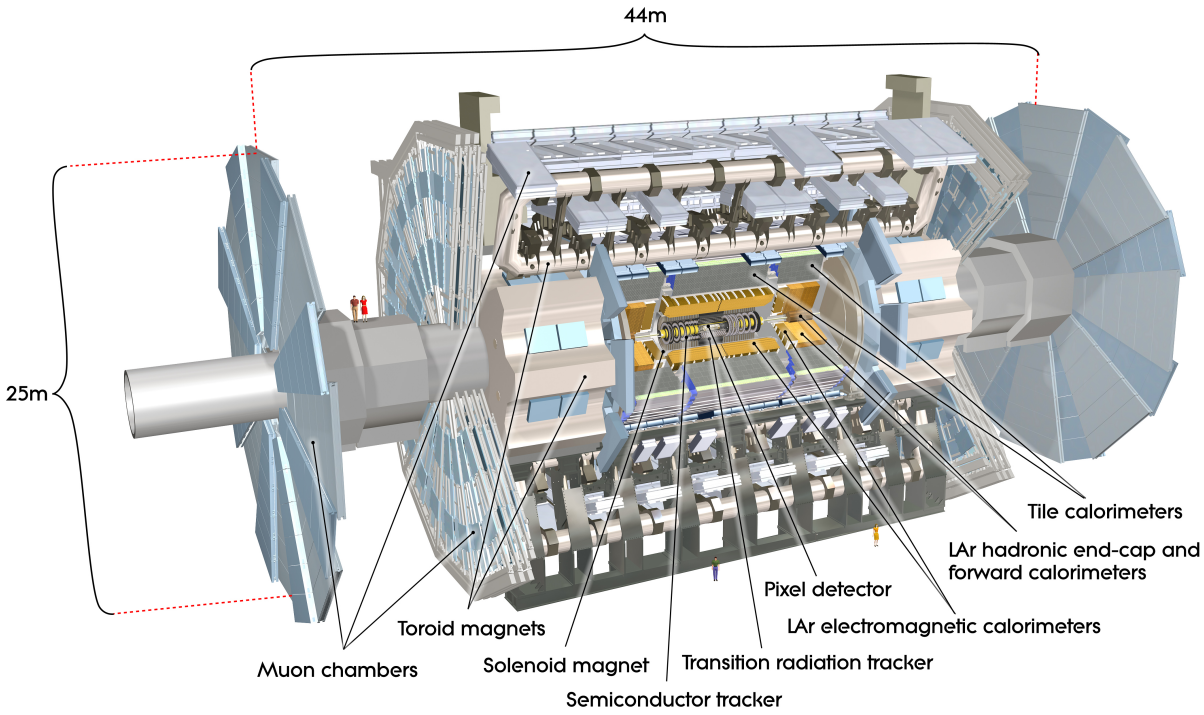


Figure 2: The ATLAS detector [1]

The tracking detectors are designed to measure the momenta of charged particles bent in a magnetic field of 2 Tesla generated by a superconducting solenoidal magnet. The pixel detector is placed as close as posible to the interaction point, to reconstruct primary vertices with high spatial resolution, followed by strip detectors in the outer layer. The electromagnetic calorimeter was designed to absorb and measure the energy of photons and electrons, the hadronic calorimeter to absorb and measure the energy of hadrons. Finally the muon spectrometer measures the muon tracks in a magnetic field of 0.5 Tesla generated by superconducting toroidal magnets.

My work is related to the silicon pixel and strip detector. As these two are situated near the interaction point of the colliding particles, they receive a high radiation dose and consequenty will suffer from radiation damage during the following years of operation. The ATLAS group at DESY is involved in the research and development of detector components for their future replacement and upgrade.

# 3 Silicon Strip and Pixel Detectors

## 3.1 Concepts

In this section I will shortly introduce some general concepts of semiconductor physics. A semiconductor is a material that has an energy gap between a valence band (full band, BV in figure 4) and a conduction band (empty band, BC in figure 4) for electrons. Semiconductors can be categorized into intrinsic and extrinsic semiconductors. The former consist of just one type of material (atoms of group IV in the periodic table) while in the latter small amounts of other elements (atoms of groups III, V; defining the semiconductors to be type-p or type-n) are added (doping).
Type-n: Atoms of group V (e.g. Phosphorus) are used to dope the silicon, so most of the free charge carriers are electrons and an additional energy level (donator level, $\epsilon_d$ in figure 4 - left) close to the conduction band is introduced. Type-p: Atoms of group III are used (e.g. Boron) to dope the silicon, so most of the free charge carriers are holes and conversely an additional energy band (acceptor level, $\epsilon_a$ in figure 4 - right) is created close to the valence band.

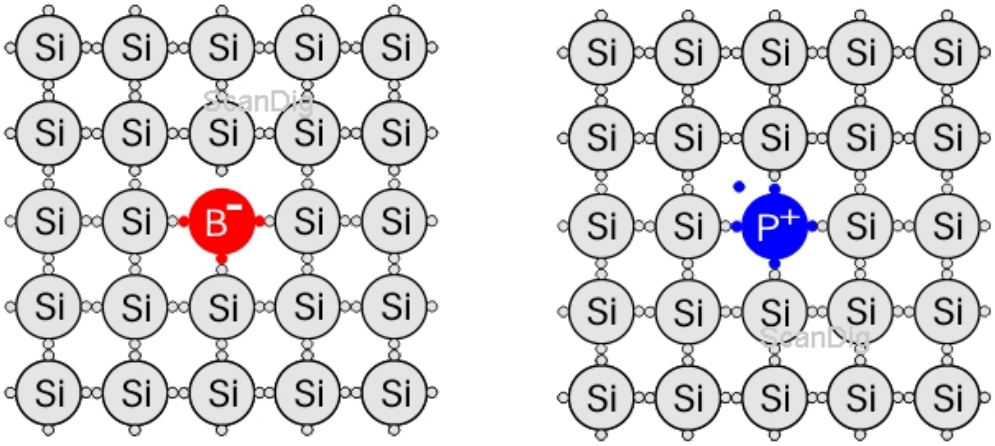


Figure 3: Ilustration of the lattice of a p-type (left) and n-type (right) semiconductor [2]

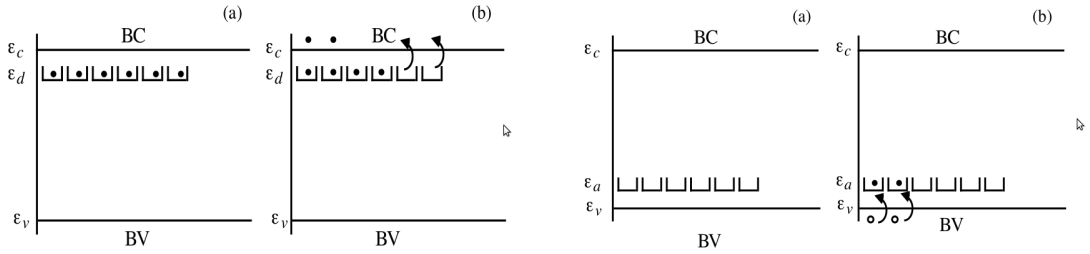


Figure 4: (a) Distribution of electrons in equilibrium state in the energy bands of the semiconductor, (b) distribution of electrons over the energy levels after a particle passing through the material in a n-type (left) and p-type (right) semiconductor [2]

## 3.2 Semiconductor Detectors

When a ionizing particle traverses semiconductor material, it generates free charge carriers (electron-hole pairs), the number being proportional to its energy loss. An externally applied electric field separates the pairs before they recombine; electrons drift towards the anode and holes to the cathode; finally the charge is collected by the electrodes (charge collection). The collected charge produces a current pulse on the electrode. The final signal is generated by a charge-sensitive preamplifier, followed by a shaping amplifier. Semiconductor detectors are popular for to their unmatched energy, spatial resolution and excellent response time.

## 3.3 Strip Detectors

One way to measure particle positions is obtained by dividing the large-area diode/sensor into many small (strip-like) regions, and read them out individually. The position of passage of the ionizing particle consequently is given by the location of the strips showing the signal.

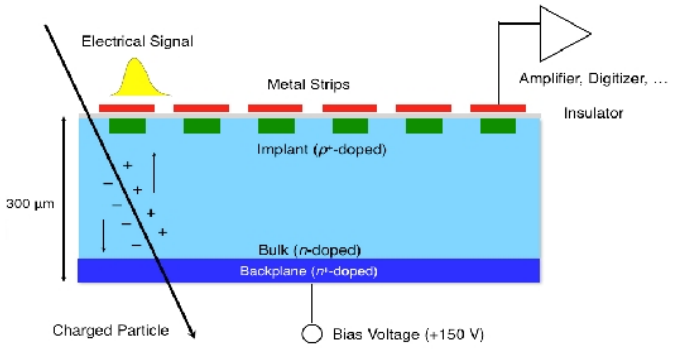


Figure 5: Strip detector, usually consists of a n-type bulk with p-type implantations, which are covered by metal segments of similar size for connecting the readout electronics

### 3.3.1 Motivation

The even higher luminosity at sLHC will lead to an increase in the number of events from 20 to 300-400 events per bunch crossing. The current ATLAS Transition Radiation Tracker (TRT) will be unable to cope with occupancy at sLHC. To keep it below a level of 1% it will be necessary to increase the number of channels in the same space.
Furthermore, the current sensors based on p-on-n technology are not sufficiently radiation hard for operation at sLHC. I have studied prototypes of the new n-on-p sensors (with better resolution and improved radiation hardness copared to the current sensors).

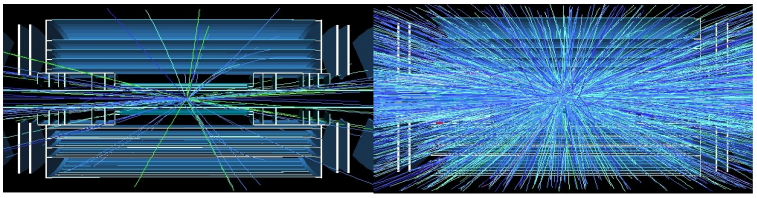

Figure 6: Illustration of particle densities at LHC (left) and sLHC (right). [3]

### 3.3.2 Measurements of sensor characteristics

The principal characteristic of the investigated sensors are:

1. produced by Hamamatsu Photonics K.K.
2. n-in-p type with p-stop isolation.
3. full-size 9.75 cm x 9.75 cm.
4. 4 rows of 1280 strips each 2.4 cm long, 5120 strips in total.

In the future it is planned to build several fully working strip detector modules to learn for future tasks in ATLAS Upgrade of the SCT endcaps. This summer I worked on the verification of the vendor specifications, characterizing and testing the following properties of the sensor:

1. **I-V characteristics:** leakage current of whole sensor and single strips
2. **C-V characteristics:** determination of full depletion voltage
3. $C_{\text{int}}$**:** Interstrip capacitance
4. $R_{\text{int}}$**:** Interstrip resistance
5. $C_{\text{cpl}}$**:** AC coupling capacitance
6. $R_{\text{bias}}$**:** Polysilicon bias resistance
7. $I_{\text{strip}}$**:** Leakage current to a strip

Figure 7: Probe Station, used to connect sensor pads with needles.

For taking these measurements a probe station was used to connect the strip sensor wire bond pads via needles to the measurement devices which then were automatically controlled and read out using a PC and a LabView program.

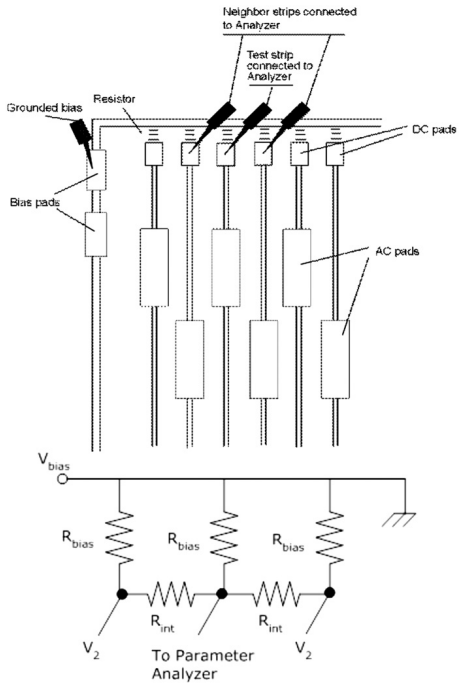


Figure 8: Illustration of strip detector connection pads

### 3.3.3 Results

The the most important, I-V and C-V measurement, are shown in figure 9 and 10.

Figure 9 shows the comparison between our own measurement (green line) and a measurement provided by the vendor (Hamamatsu, black line) of the I-V-characteristics (leakage current over depletion voltage) of the whole sensor. Both measurements are in good agreement. Using the slope of the curve in its linear region (blue line) we can estimate the silicon bias resistance (1.17 MΩ).

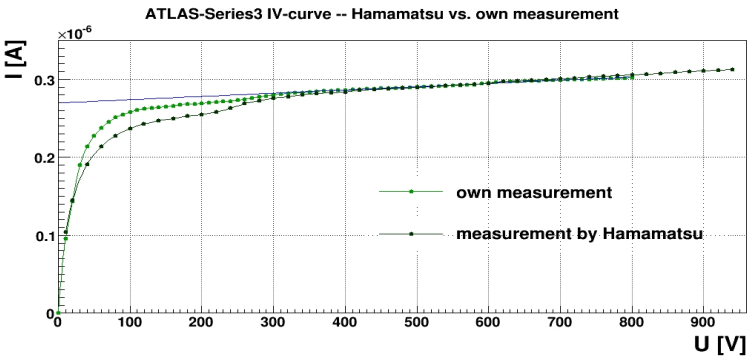


Figure 9: I-V measurements

Figure 10 shows the C-V characteristic (capacitance over depletion voltage) plotted in a double logarithmic scale. Using power law fits for the two linear regions of the measured curve (blue lines) the depletion voltage can be estimated by calculating the voltage at the crossing point of the two fits (295 V).

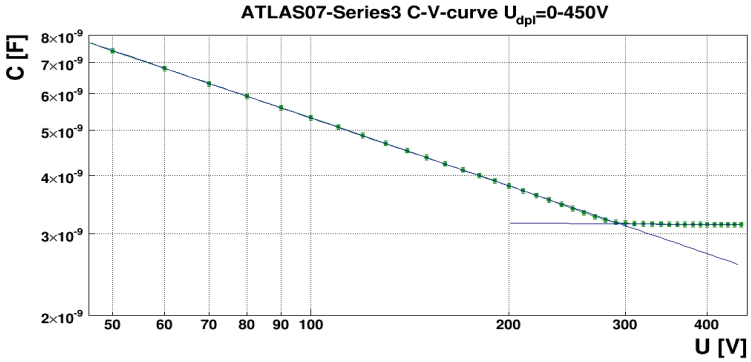


Figure 10: C-V measurements

Apart from these measurements, which describe characteristics of the sensor as a whole, several other properties of individual strips have been investigated. The results of these and a comparison to the design specifications are given in Table 1. Due to the lack of an automated probe station it was not possible to measure all the characteristics mentioned above in a systematic way for all the 1280 strips per row of the whole sensor.

| | ATLAS07 specifications | Measurement |
|---|---|---|
| Leakage Current | $< 200\mu$A at 600V | $\sim 0.3\mu$A at 600V |
| Full Depletion Voltage | $< 500$V | 295V |
| Coupling Capacitance at 1kHz | $> 20p$F/cm | Tested* |
| Silicon Bias Resistans | $1.5 \pm 0.5$MΩ | 1.17MΩ |
| Current through dielectric | $I_{\text{diel}} < 10n$A | Not Tested (destructive) |
| Strip Current $I_{strip}$ | No explicit limit | Tested* |
| Inter-Strip Capacitance | $< 1.1p$F/cm | Tested* |
| Inter-Strip Resistance | $> 10 \times R_{\text{bias}} \sim 15$MΩ | Not Tested* |

*automatic probe station is needed to reliably measure this characteristic.

Table 1: Comparison between own measurements and desing specification of the sensor

## 3.4 Pixel Detectors

Pixel detectors are based on the same principle as strip detectors but with the semiconductor diode being devided into elements of very small rectangular two-dimensional shape. The large number of such detector elements on the sensor surface ensures high spatial resolution in two coordinates.

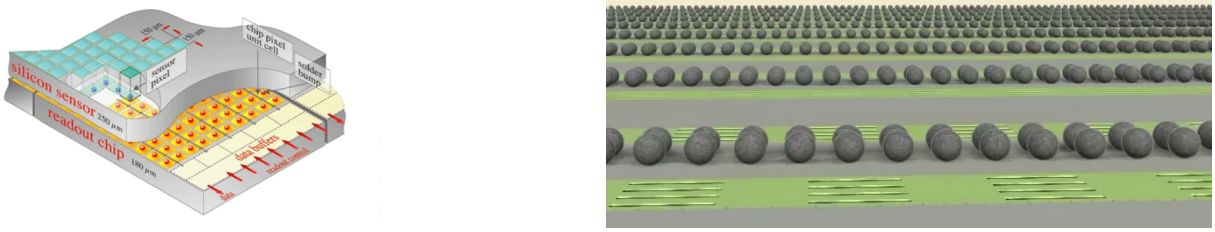


Figure 11: Schematic of a pixel detector (left) [4]. The readout chip is directly conected to the sensor elements via bump bonds (right) [1].

### 3.4.1 Motivation

For the development of new detector components it is cruicial to identify and quantify possible sources of influence on their operation, e.g. impact on the readout noise of sensor modules.
Especially the introduction of new powering schemes like DC-DC powering, needs prior investigation, as DC-DC converters, usually being switching devices, generate alternating currents in the powering cables of the front-end electronics. It is important to know their influence on the measurements (increase in readout noise) and within which frecuency range these effects are crucial. If known the converters switching frecuency can be choosen accordingly to minimize the noise. Therefore we investigated the susceptibility of the front-end electronics of a pixel detector to conductive noise of certain amplitude and frequency.

### 3.4.2 Noise susceptibility measurements

Figure 12 shows the experimental setup used to take the measurements described above. In the botton left shielding box we can see a coil, with which alternating currents (generated by a function generator) were induced into the powering lines of the pixel front-end electronics. In the lower right box we can see the USBPix system used for the readout and communication with a single chip board (shown in the upper right box), which hosts a single pixel front-end chip (FE-I3) attached to a small pixel sensor. This front-end IC is the same as used on the modules of the current ATLAS pixel detector.

While injecting the currents we used a oscilloscope to measure the current and voltage of the noise signal in the affected powering line.
To readout the pixel data, we used the STcontrol software package for the USBPix readout system, which allows the measurements and visualization of the noise levels, i.e. equivalent noise charge (ENC counts), for each individual pixel or pixel type.

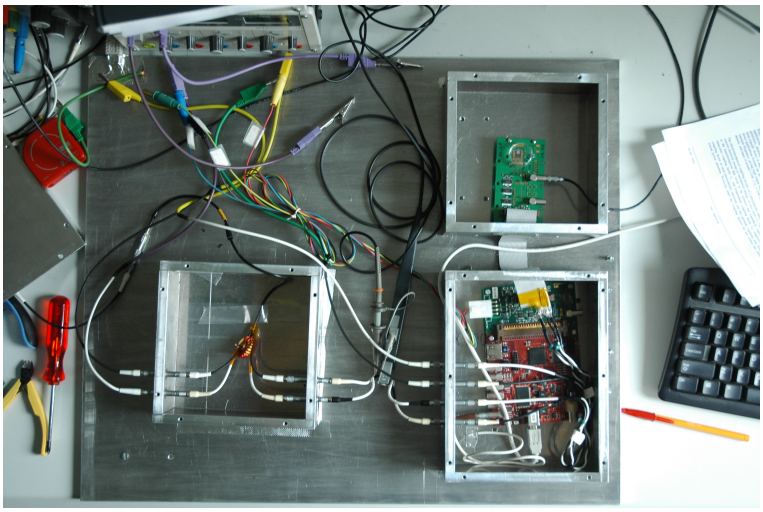

Figure 12: USBPix experimental setup.

### 3.4.3 Results

This part summarizes the results obtained from the measurements described before.
First of all the noise of the readout was measured without applying noise currents on the powering lines.
The pixel detector is powered through four different cables, two for the digital part (VDDD, DGND) and two for the analog part (VDDA, AGND), and so for the charge sensitive amplifiers in the readout cells of the front-end chip. Noise currents were induced into all four lines seperately (differential mode noise) and into both lines of the analog / digital part at the same time (common mode noise).

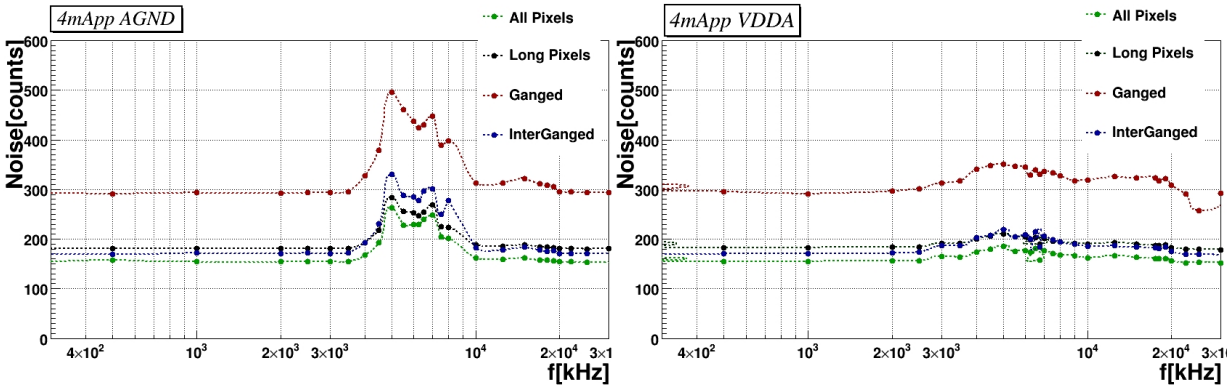


Figure 13: Readout noise when inducing differential mode noise currents (4 mA) into the powering lines of the analog part over frecuency of the injected noise signal.

Figures 13, 14 and 15 show the results of the measurements of the readout noise in ENC counts over the frequency of the injected noise signal. As expected, the most sensitive part on the pixel front-end electronics is the analog part, because the analog ground (AGND) is used as a reference voltage for the amplifier.
The DC-DC converters currently under investigation use frequencies in the range of 500-1000 kHz, which is far away from the sensitive region of the pixel front-end electronics.

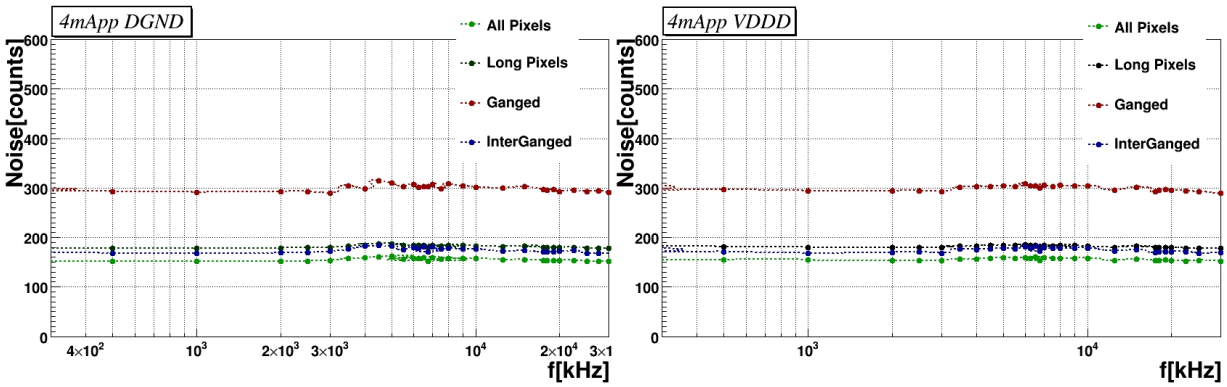


Figure 14: Readout noise when inducing differential mode noise currents (4 mA) into the powering lines of the digital part over frecuency of the injected noise signal.

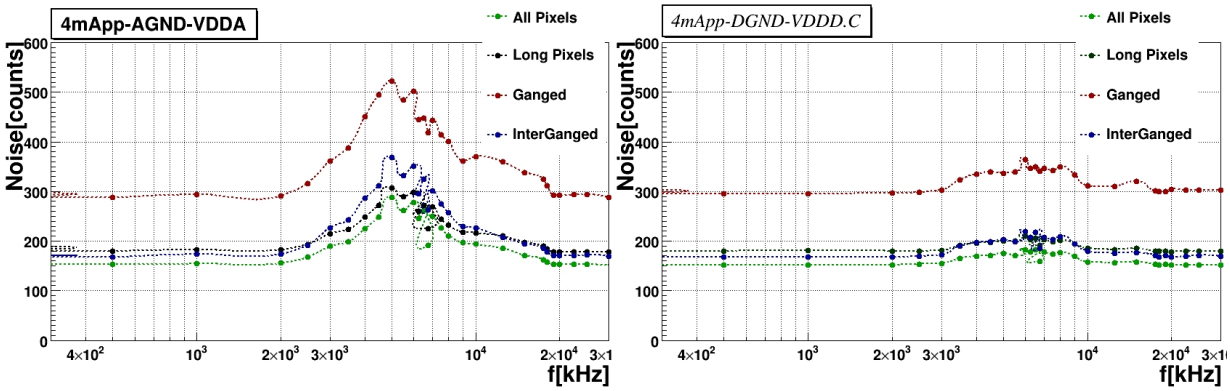


Figure 15: Readout noise when inducing common mode noise currents (4 mA) into the powering lines of the digital / analog part over frecuency of the injected noise signal.

The experience and knowledge gained from these tests can be easily transferred to future similar measurements of strip detectors.

## 3.5 DC-DC powering

### 3.5.1 Motivation

The future ATLAS upgrade involves an increase in the number of readout channels and number of detector modules. Nowadays power is transferred at approximately 2V on two individual cable pairs to each individual module. It will be inevitable to switch to an alternative powering scheme, as it will be impossible to put more cables inside the designated spaces. One solution is to transfer power at high voltage (i.e. 12V) to a group of modules, and convert the voltage locally. For this purpose it is planned to use conventional DC-DC, i.e. buck converters attached to each individual module, which convert the high voltage down to the supply voltage needed by the frond-end electronics. Another advantage of this scheme is its higher overall efficiency, as the power dissipation in the cables is smaller ($P = RI^2$) and the load to the cooling system will decrease.
To keep the material budget inside the tracker as low as possible, size and material of the converters have to be optimized, too. To achieve this, apart from conventional DC-DC

converters, more recent technologies like piezoelectric transformers have been investigated, as they show several advantages over conventional converter types.

### 3.5.2 Impedance measurements of piezoelectric ceramics

Piezoelectrical materials develop an electric field when mechanically stressed (piezoelectric effect, figure 16), and develop a strain upon the application of an electric field (invese piezoelectric effect, figure 16).
Unlike conventional magnetic DC-DC converters, piezoelectric transformers convert AC voltage at the primary side to a proportional voltage at the secondary side. While con-

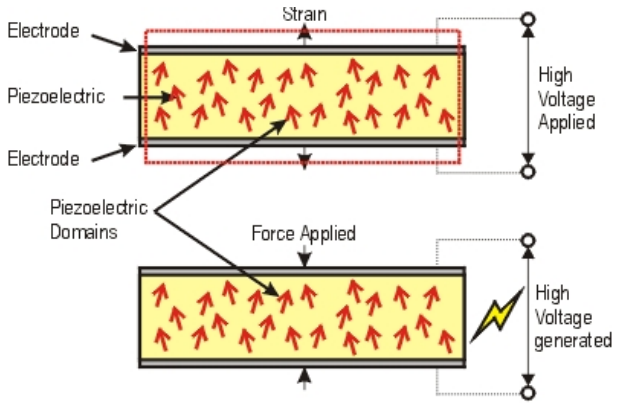


Figure 16: Piezoelectric effect [5]

ventional magnetic transformers use the electromagnetic coupling between a primary and secondary coil, piezoelectric transformers use the mechanical coupling between two piezoelectric materials.
Due to the high energy density of piezoelectric transformers, these converters can be very compact and light compared to conventional DC-DC converters. But, because piezoelectric transformers behave like a resonant band-pass filter, high efficiency is only reached when operating them close to the resonance frecuency, and driver circuits are more complicated.
For the development of such a driver circuit, the dependence of the impedance from the frequency around the ceramics resonance frecuency was studied with a piezoelectric transformer manufactured by NEC-Tokin.

### 3.5.3 Results

As described, the piezoelectric transformer itself consists of two coupled pieces of piezoelectric ceramics with pairs of connections for its (AC) input and output. A first characterization of the properties of the device can be obtained by measuring the impedance at its input/output. For this we connected a function generator to the input (output), applying sinusoidal signals of different frecuency in a range around the device's resonance frecuency. Meanwhile the current, voltage and the phase were measured with an oscilloscope, while the remaining output (input) terminals were shorted.
From this we can calculate the impedance using $|z| = u/i$ and phase shift around the transformer resonance frequency, figure 17.

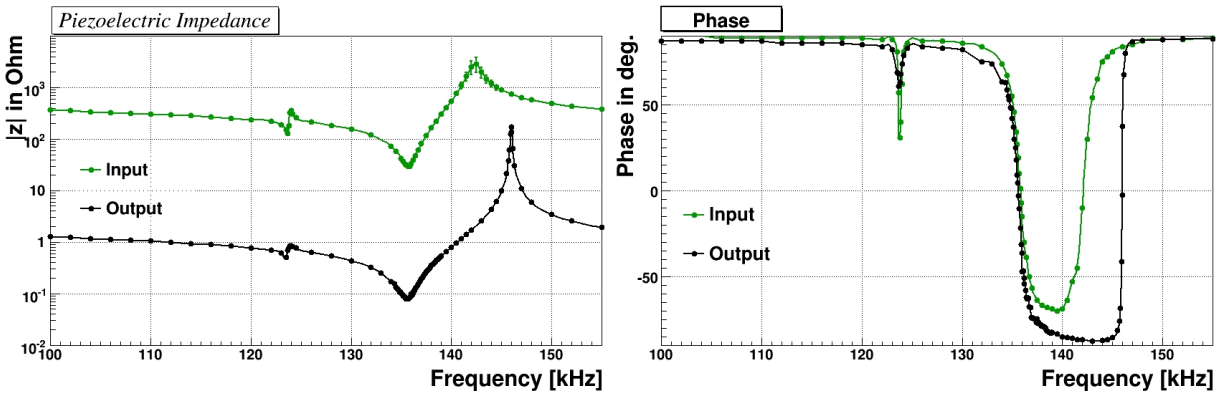


Figure 17: Impedance (left) and phase shift (right) as a function of the signal frequency for input and output side

From these measurements values for the simulation (equivalent circuit) of the piezoelectric transformer can be obtained, which are planned to be used for the design of a driver and control circuit for these devices.

# 4 Conclusions

The development of detector components for ATLAS requires many years of research and developement before being installed and reliably operated. Therefore ATLAS as a whole is the result of the work of approximately 3000 scientists and engineers from 150 universities and laboratories all over the world, each of them contributing in many aspects and details, bringing the whole project to perfection.

Even though the LHC and the ATLAS detector have been running reliably and taking data efficiently for several month now, research and development for its upgrade in approximately 10 years have already started.

Although the research topics I have been working on were presented independently is this report, they are strongly linked. The need to increase the resolution of the tracker for the operation at sLHC creates problems like insufficient efficiency and space inside the detector (e.g. for routing all powering cables). The most viable solution to overcome these problems is to power the detector modules in groups, by converting the current locally, directly inside the detector using DC-DC converters. As these converters generate noise in the cables, their influence on the detector electronics has to be characterized, so the measurements are not affected.

To gain first impressions of possible influences of the converters switching noise, the susceptibility of actual ATLAS pixel readout electronics to noise currents on its powering lines has been investigated and sensitive frequency ranges have been identified. As in the upgraded ATLAS detector many detector parts will be exchanged, this type of measurements has to be repeated with the future hardware to provide reliable estimates for the components to be installed.

With respect to the Semiconductor strip detector, for these (and many other) investigations the construction of several fully functional strip detector modules is planned by the ATLAS group. The silicon strip sensors themselves constitute the main component of the detector modules. Their main characteristics were measured and compared with the vendor's specifications.

Concerning the inevitable changes to the powering system for the tracker part, one of the alternative schemes currently in discussion, DC-DC powering, is topic of investigation within the ATLAS group. As a future compact alternative for the well established and widely used inductor based (buck) DC-DC converters, piezoelectric transformers have been investigated during my stay. Measurements of the input/output impedance of piezoceramics were taken, which will be used to calculate values for equivalent circuits of these and facilitate the simulation and development of driver and control circuits for a final converter.

# References


[1] http://cdsweb.cern.ch/

[2] José.A.Manzanares. *Física del Estado Solido*. Facultat de Física, Universitat de València 2009/2010

[3] http://atlas.web.cern.ch/Atlas/GROUPS/UPGRADES/

[4] http://cms.web.cern.ch/cms/index.html

[5] http : //www.azom.com/work/W3RUE3K9c3NUAjqa9j78$_{\text{f}}$iles/image002.gif

[6] Y.Unno, et al. *Developement of n-on-p silicon sensors for very high radiation environments*. Nuclear Instruments and Methods in Physics Research A (2010), doi:10.1016/j.nima.2010.04.080.

[7] E.L. Horsley, M.P. Foster, D.A. Stone. *State-of-the-art Piezoelectric Transformer Technology*. Proc. European Conference on Power Electronics and Applications 2007, Aalborg, Denmark.

[8] Manh Coung Do. *Piezoelectric Transformer Integration Possibility in High Power Density Applications*. Ph.D Thesis, University Dresden, 2008

[9] Gerhard Lutz. *Semiconductor Radiation Detectors*. Springer,1999


# 5 Acknowledgements


I have to thank all of the people I met, because from the first day, when I arrived here, and each step than I took, I was always found the best person possible. Thanks to everyone at DESY for making my stay very pleasant.

Special thanks to Conrad Friedrich and Hongbo Zhu for all the help that they have given me to succeed in my work. I also want to thank Ulrich Husemann for letting me participate in his group.

I want to thank all for having patience with my English, especially Matteo and Juan Pablo for your improvising English classes.

So: Moltes Gracies (Thank you very much)